A COUPLE OF MY "FAVORITE" TJH PAPERS AND THEIR CONTINUING SIGNIFICANCE

Mark J McCready
University of Notre Dame

IN CASE I DON'T LOOK FAMILIAR

Mark J. McCready

Turbulent Mass Transfer Rates to a Wall for Large Schmidt Numbers

DUDLEY A. SHAW
and
THOMAS J. HANRATTY
University of Illinois
Urbana, Illinois

New measurements are presented on the influence of Schmidt number on the rate of mass transfer between a turbulent fluid and a pipe wall. It is found that for large Schmidt numbers the fully developed mass transfer coefficient is related to the friction velocity and the Schmidt number by the equation

$$K_{\infty} = 0.0889\, v^{*}\, Sc^{-0.704}$$

The experiments are accurate enough to rule out the $Sc^{-2/3}$ or the $Sc^{-3/4}$ relations commonly used, deduced from plausible limiting expressions for the eddy diffusivity close to a wall. It is argued that these expressions are valid only over a vanishingly small portion of the concentration field as $Sc \to \infty$.

J. Fluid Mech. (1971), *vol.* 50, *part* 1, *pp.* 107–132 107
Printed in Great Britain

Weak quadratic interactions of two-dimensional waves

By YOUNG YUEL KIM AND THOMAS J. HANRATTY
Department of Chemical Engineering, University of Illinois, Urbana, Illinois

(Received 9 April 1970 and in revised form 24 February 1971)

FAVORITE PAPER #1

J. Fluid Mech. (1971), vol. 50, part 1, pp. 107–132 107
Printed in Great Britain

Weak quadratic interactions of two-dimensional waves

By YOUNG YUEL KIM AND THOMAS J. HANRATTY
Department of Chemical Engineering, University of Illinois, Urbana, Illinois

- "Wind" (linear process) tries to create a most favored wavelength ~ 1-3 cm: Where do all of the rest of the waves come from?

transition.

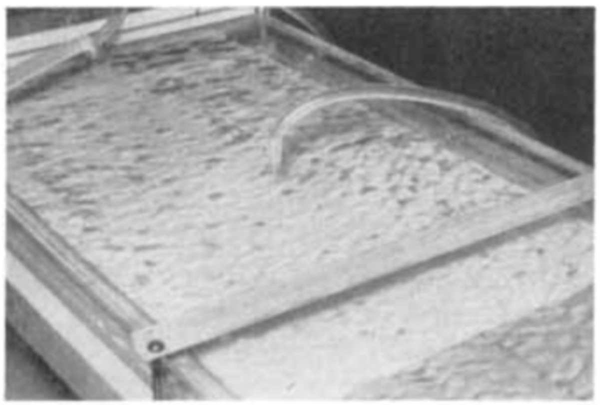

Fig. 6. Photograph of squall surface.

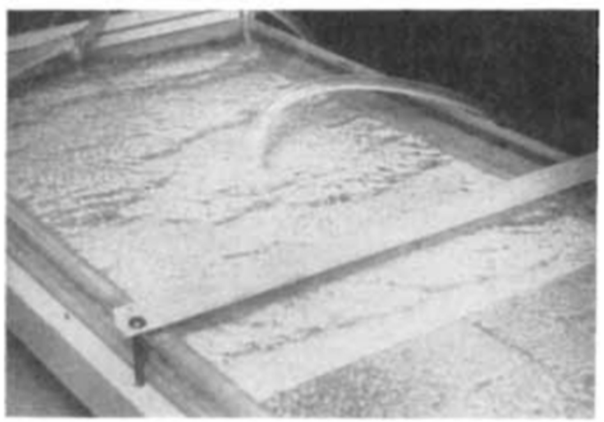

Fig. 7. Photograph of roll waves.

Interaction Between a Turbulent Air Stream and a Moving Water Surface

THOMAS J. HANRATTY and JAMES M. ENGEN
University of Illinois, Urbana, Illinois

K&H: FORMULATION WAS NOVEL

- Researchers in the geophysical world had examined the problem and had concentrated on situations of perfect "resonance" —
- special selections of wavelengths of 2 or 3 waves (effectively a collection of overtones) where one of the group could excite others.
    - The pitch of a violin string, or any musical instrument for that matter is a collection of overtones that result from an "forcing" at one of them with "energy" transferring between them
- **K&H approach allowed for <u>imperfect</u> resonance — which is the most prominent energy transfer mechanism.**

EQUATIONS

$$\eta = \sum_{\alpha=0}^{N} A_\alpha e^{i\alpha\theta} + A_\alpha^* e^{-i\alpha\theta}, \qquad (2)$$

$$\Phi = \sum_{\alpha=1}^{N} B_\alpha \frac{\cosh \alpha k(y+h)}{\sinh \alpha kh} e^{i\alpha\theta} + \text{complex conjugate}, \qquad (3)$$

$$-T\frac{\partial^2\eta}{\partial x^2} + g\eta - \frac{\partial\Phi}{\partial t} - \frac{\partial^2\Phi}{\partial t\,\partial y}\eta + \frac{1}{2}\left\{\left(\frac{\partial\Phi}{\partial x}\right)^2 + \left(\frac{\partial\Phi}{\partial y}\right)^2\right\} = 0,$$

$$\frac{\partial\eta}{\partial t} - \frac{\partial\Phi}{\partial x}\frac{\partial\eta}{\partial x} + \frac{\partial\Phi}{\partial y} + \frac{\partial^2\Phi}{\partial y^2}\eta = 0,$$

$$\left.\begin{aligned}
A_{1,\xi} &= 4ik(P_1A_1^*A_2 + P_2A_2^*A_3 + P_3A_3^*A_4) = \text{right-hand side of (1)},\\
A_{2,\xi} &= iL_2A_2 - 2ik(P_4A_1^2 + P_5A_1^*A_3 + P_6A_2^*A_4) = \text{right-hand side of (2)},\\
A_{3,\xi} &= iL_3A_3 - \tfrac{4}{3}ik(P_7A_2A_1 + P_8A_1^*A_4) = \text{right-hand side of (3)},\\
A_{4,\xi} &= iL_4A_4 - ik(P_9A_1A_3 + P_{10}A_2^2) = \text{right-hand side of (4)},
\end{aligned}\right\}$$

where $\omega^2 = (gk + k^3T)\tanh(kh),$

$$L_\alpha = \frac{\alpha}{2} - \frac{gk + \alpha^2k^3T}{2[\alpha K]\,\omega^2}$$

$$\left.\begin{aligned}
P_1 &= (1/8[K])([K]^2 + 4[K][2K] - 3),\\
P_2 &= (1/8[K])(2[K][2K] + 3[K][3K] + 6]2K][3K] - 7),\\
P_3 &= (1/8[K])(4[K][4K] + 3[K][3K] + 12[3K][4K] - 13),\\
P_4 &= ([K]/[2K])P_1,\\
P_5 &= (1/8[2K])(4[K][2K] + 12[2K][3K] + 6[K][3K] - 14),\\
P_6 &= (1/8[2K])(8[2K]^2 + 32[2K][4K] - 24),\\
P_7 &= (1/8[3K])(9[K][3K] + 6[K][2K] + 18[2K][3K] - 21),\\
P_8 &= (1/8[3K])(9[K][3K] + 12[K][4K] + 36[3K][4K] - 39),\\
P_9 &= (1/8[4K])(16[K][4K] + 48[3K][4K] + 12[K]3[K] - 52),\\
P_{10} &= (1/8[4K])(32[2K][4K] + 8[2K]^2 - 24).
\end{aligned}\right\}$$

THE EQUATIONS

- This was done for the case of no viscosity and also approximately for weak viscosity — to show wave decay as well as interactions.
- Oh.. they also did experiments that showed the evolution of waves and the formation of different sets of overtones even when the waves were not perfectly resonant.

FIGURES FROM KIM'S THESIS

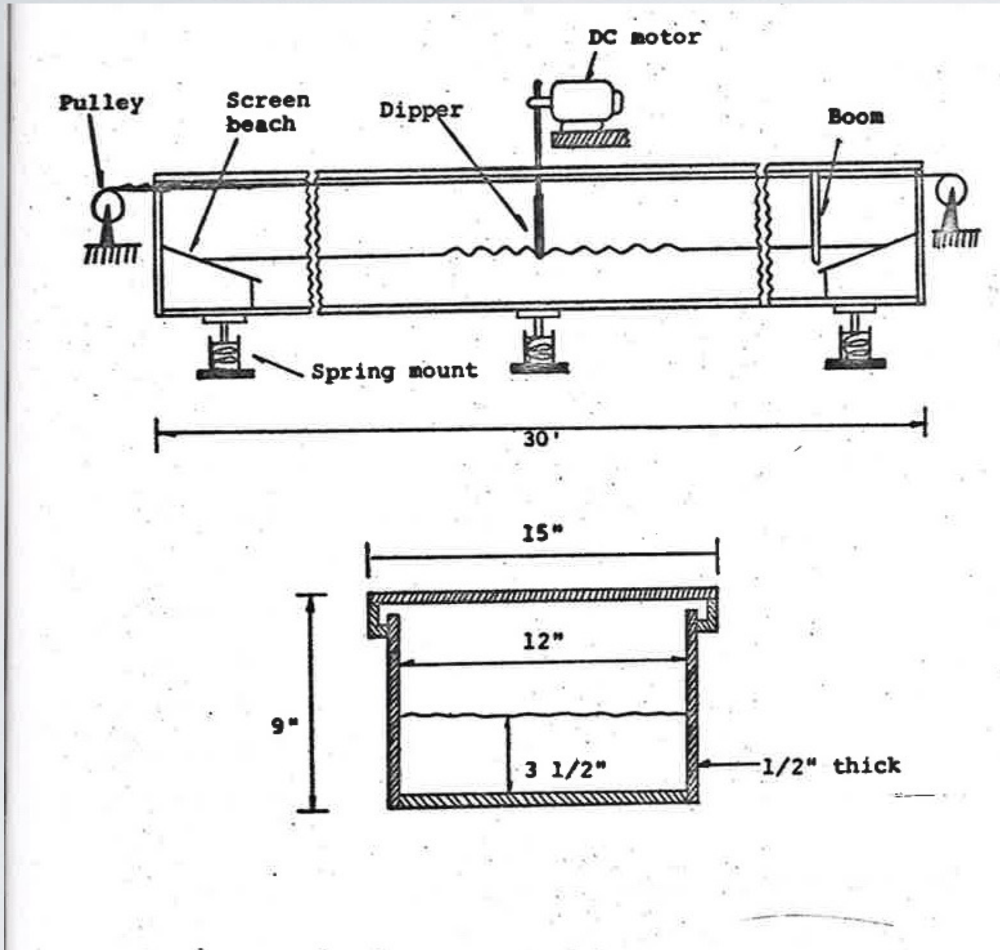

Figure 14. Schematic diagram of wave tank

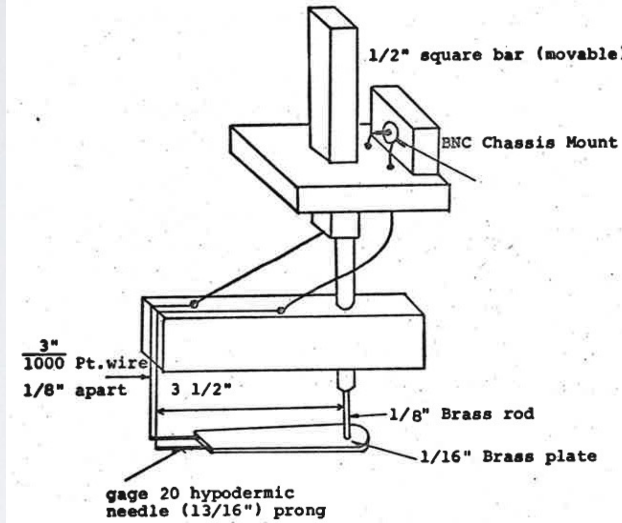

Figure 16. Resistance probe for shallow water wave measurements

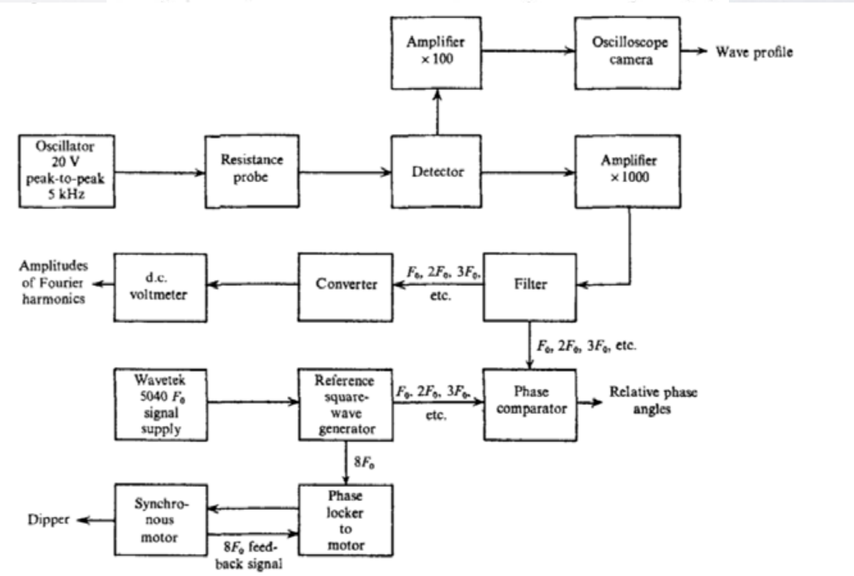

FIGURE 5. Schematic diagram for wave measurements.

EXPERIMENTS: CONFIRM BASIC PREMISE

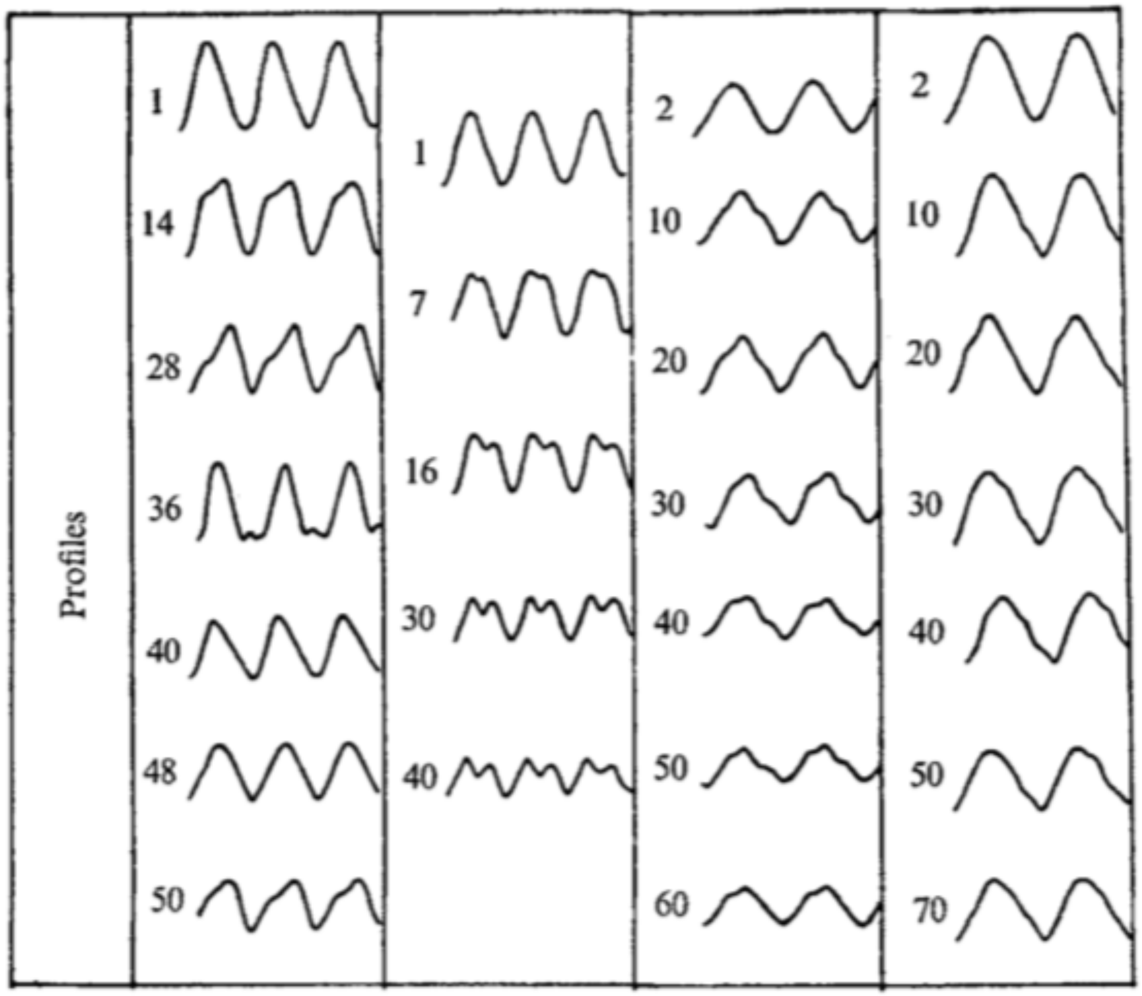

c/s	10·46	9·96	8·40	7·57
n	1·76	1·98	2·99	4·02
°C	25·4	29·1	24·0	26·1
ka_1	0·045	0·061	0·049	0·063

FIGURE 6. Changes of wave profiles on deep water as functions of distance from the wave maker.

EXPERIMENTS: THEORY IS QUANTITATIVELY CORRECT

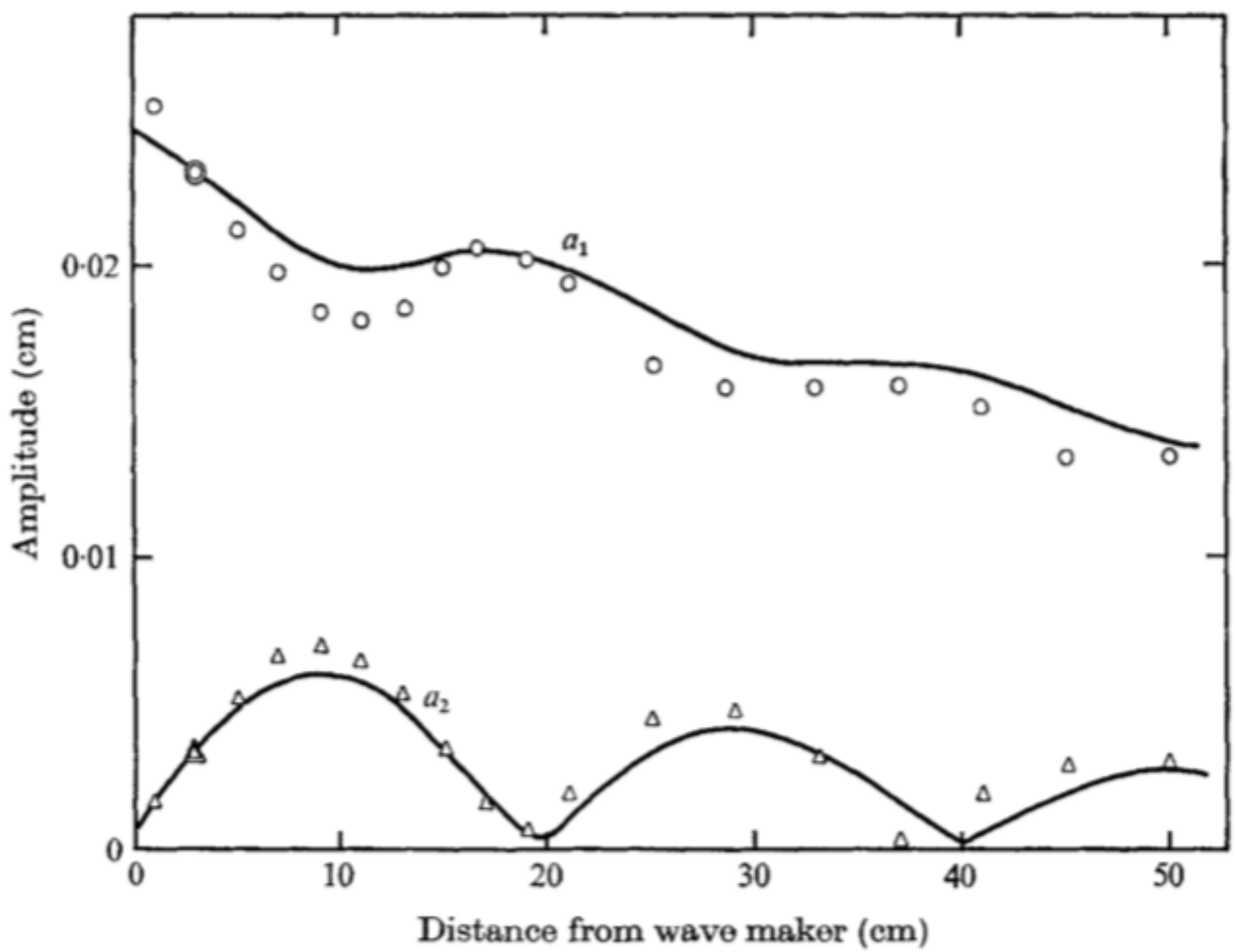

FIGURE 7. Observed variations of Fourier harmonics for $n = 1{\cdot}41$ (11·48 c/s), $\epsilon = ka_1 = 0{\cdot}0793$, temperature = 26·2 °C. ——, predicted; ○, △, measured.

FOLLOW UP

- We studied waves for more than 20 years. Our nonlinear theories followed the basic ideas of Kim and Hanratty, augmented by advances in nonlinear dynamics and numerical spectral techniques.
  - But the nonlinear coefficients on the quadratic terms match K&H for sufficiently high Reynolds numbers.
  - Work previous to K&H, that had relied on exact resonance, could not be extended to deal with a complete spectrum of waves

ANALYSIS: UPDATED VERSION OF KIM AND HANRATTY

Stabilization mechanisms of short waves in stratified gas–liquid flow

Massimo Sangalli, Mark J. McCready, and Hsueh-Chia Chang
Department of Chemical Engineering, University of Notre Dame, Notre Dame, Indiana 46556

$$\mathbf{\Phi}'(x,y,t)=\sum_{n=-\infty}^{\infty}\sum_{m=1}^{\infty}A_{mn}(t)\,\boldsymbol{\phi}_{mn}(y)\exp(in\alpha x), \quad (28)$$

$$\left(\mathscr{M}\frac{\partial}{\partial t}-\mathscr{L}\right)\mathbf{\Phi}'=\mathscr{N}(\mathbf{\Phi}'), \quad (10)$$

$$\begin{aligned}\dot{A}_1=&\lambda_1A_1+(2\mathbf{D}(\mathbf{f}_2e^{i2\alpha_1x},\bar{A}_1\bar{\mathbf{w}}_1),\mathbf{v}_1)\\&+(2\mathbf{D}(\mathbf{f}_0,A_1\mathbf{w}_1),\mathbf{v}_1)\\&+(3\mathbf{T}(A_1\mathbf{w}_1,A_1\mathbf{w}_1,\bar{A}_1\bar{\mathbf{w}}_1),\mathbf{v}_1), \quad (34)\end{aligned}$$

where tensors **D** and **T** as defined from the nonlinear vector function $\mathscr{N}$ in (10)

$$\mathbf{D}(\Phi_1,\Phi_2)=\frac{1}{2}\frac{\partial^2}{\partial\delta_1\partial\delta_2}\mathbf{N}(\delta_1\mathbf{\Phi}_1+\delta_2\mathbf{\Phi}_2)\big|_{\delta_1=\delta_2=0},$$

$$\mathbf{T}(\Phi_1,\Phi_2,\Phi_3)=\frac{1}{3!}\frac{\partial^3}{\partial\delta_1\partial\delta_2\partial\delta_3}\mathbf{N}(\delta_1\mathbf{\Phi}_1+\delta_2\mathbf{\Phi}_2+\delta_3\mathbf{\Phi}_3)\big|_{\delta_1=\delta_2=\delta_3=0}$$

MECHANISMS AT PLAY IN WIND-GENERATED WAVES

Phys. Fluids, Vol. 9, No. 4, April 1997

Sangalli, McCready, and Chang

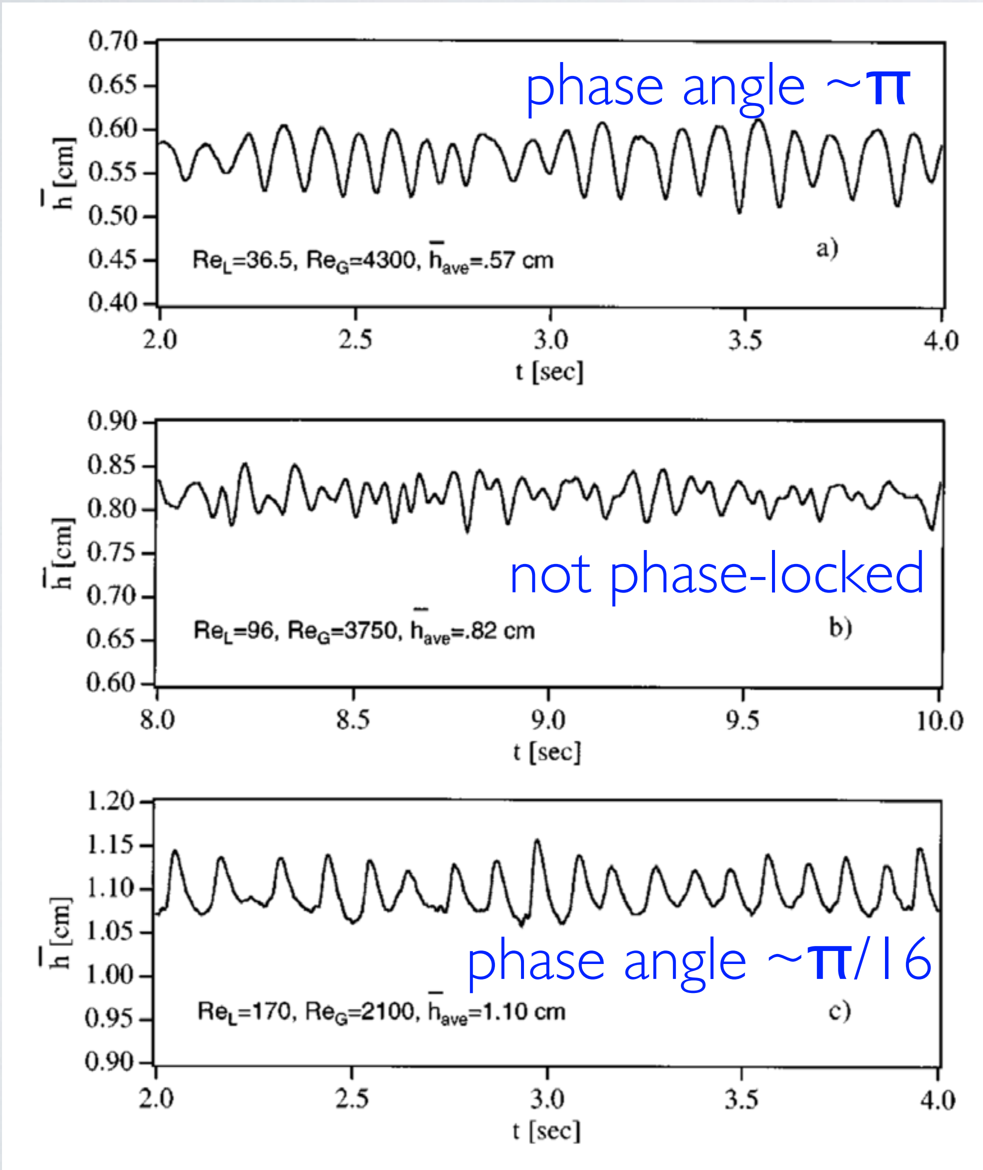

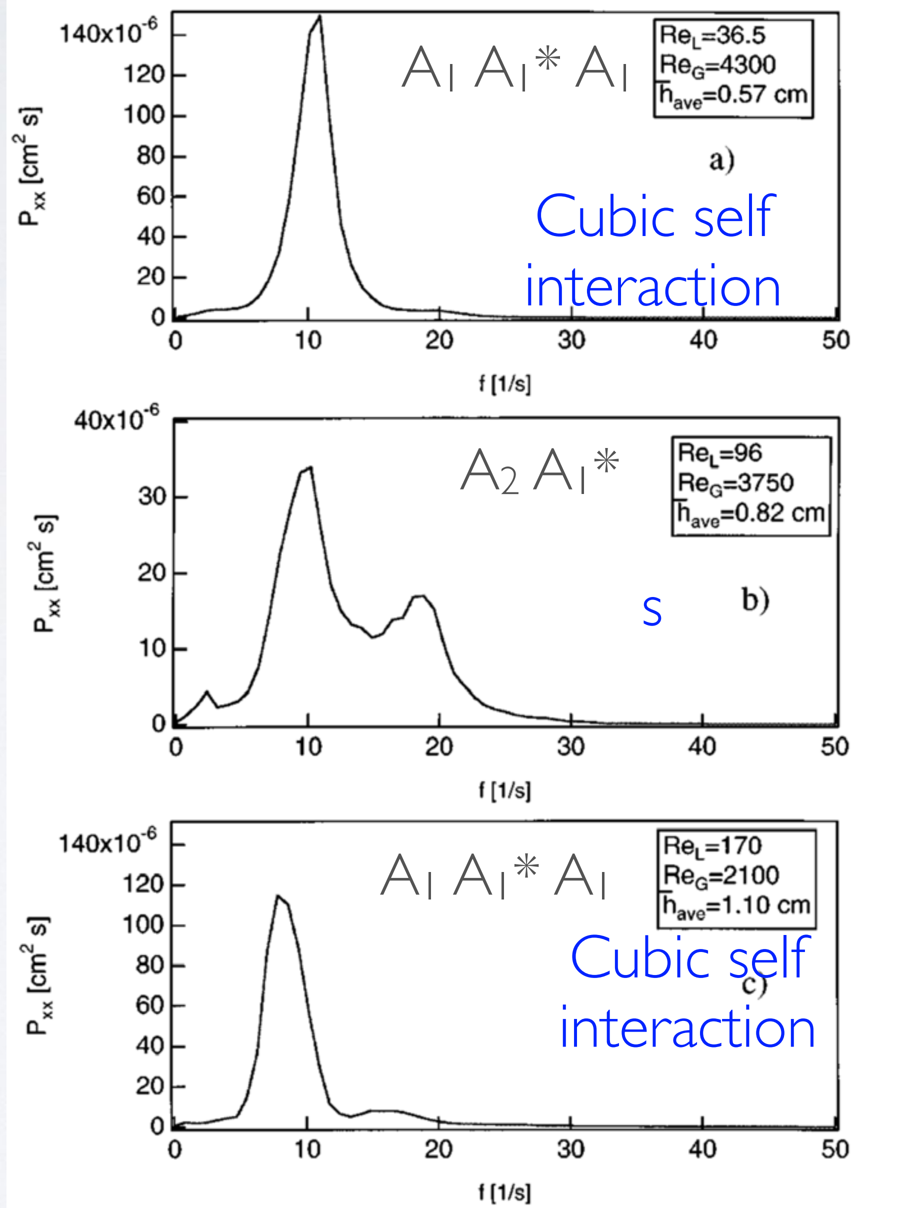

SIMULATION OF WAVE SPECTRUM

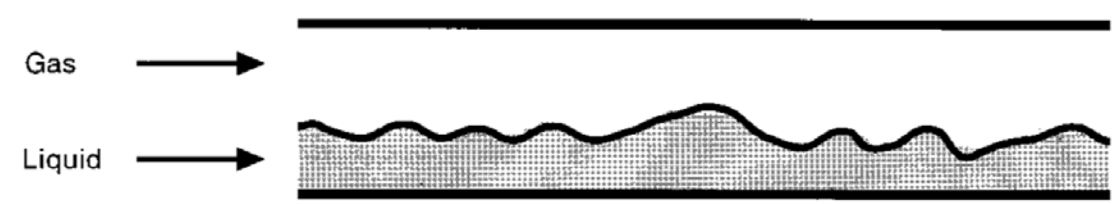

FIG. 1. Schematic of the channel for gas–liquid Poiseuille flow.

$$\dot{A}_{nl}=\lambda_{nl}A_{nl}+\sum_{p,q,r,s} q_{nl,pr,qs}A_{pr}A_{qs} + \sum_{p,q,m,r,s,z} t_{nl,pr,qs,mz}A_{pr}A_{qs}A_{mz}.$$

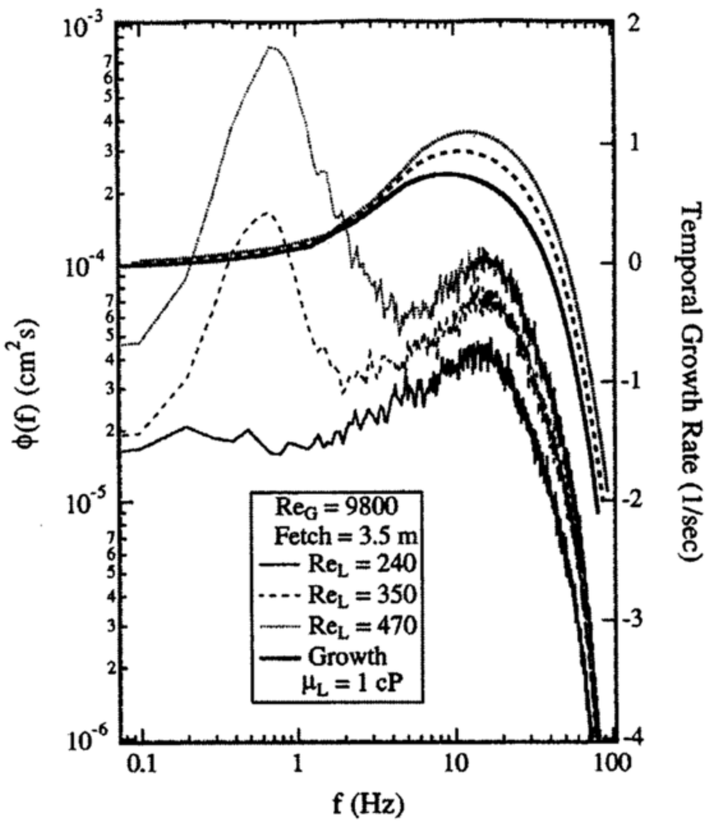

FIG. 1. Measured power spectra from a 2.54 cm, rectangular air–water channel. $Re_G=9800$, $Re_L=240–470$. Data are compared to growth rates from linear theory.

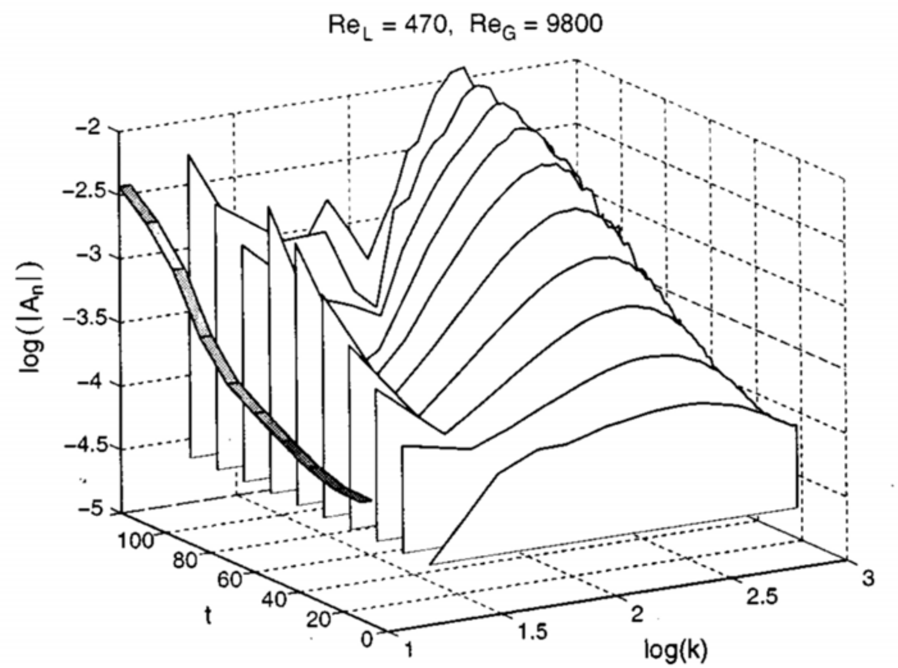

FIG. 3. Air–water simulation for $Re_G=9800$, $Re_L=470$. The amplitude of the mean flow mode, subject to the FVF condition, is plotted to the left of spectra. Note the emergence of a low wave number wave, in agreement with the experimental measurements of Fig. 1.

MATCHED DENSITY, VERTICAL INTERFACE TWO-LAYER FLOW

WAVE MAP FOR ROTATING COUETTE FLOW EXPERIMENT

GALLAGHER, LEIGHTON AND MCCREADY, *PHYS. FLUIDS*, 1997

LEFT OF THE LINE, ONLY SHORT WAVES ARE UNSTABLE

REGIONS OF "NO WAVES" EXIST WHERE LONG WAVES ARE UNSTABLE

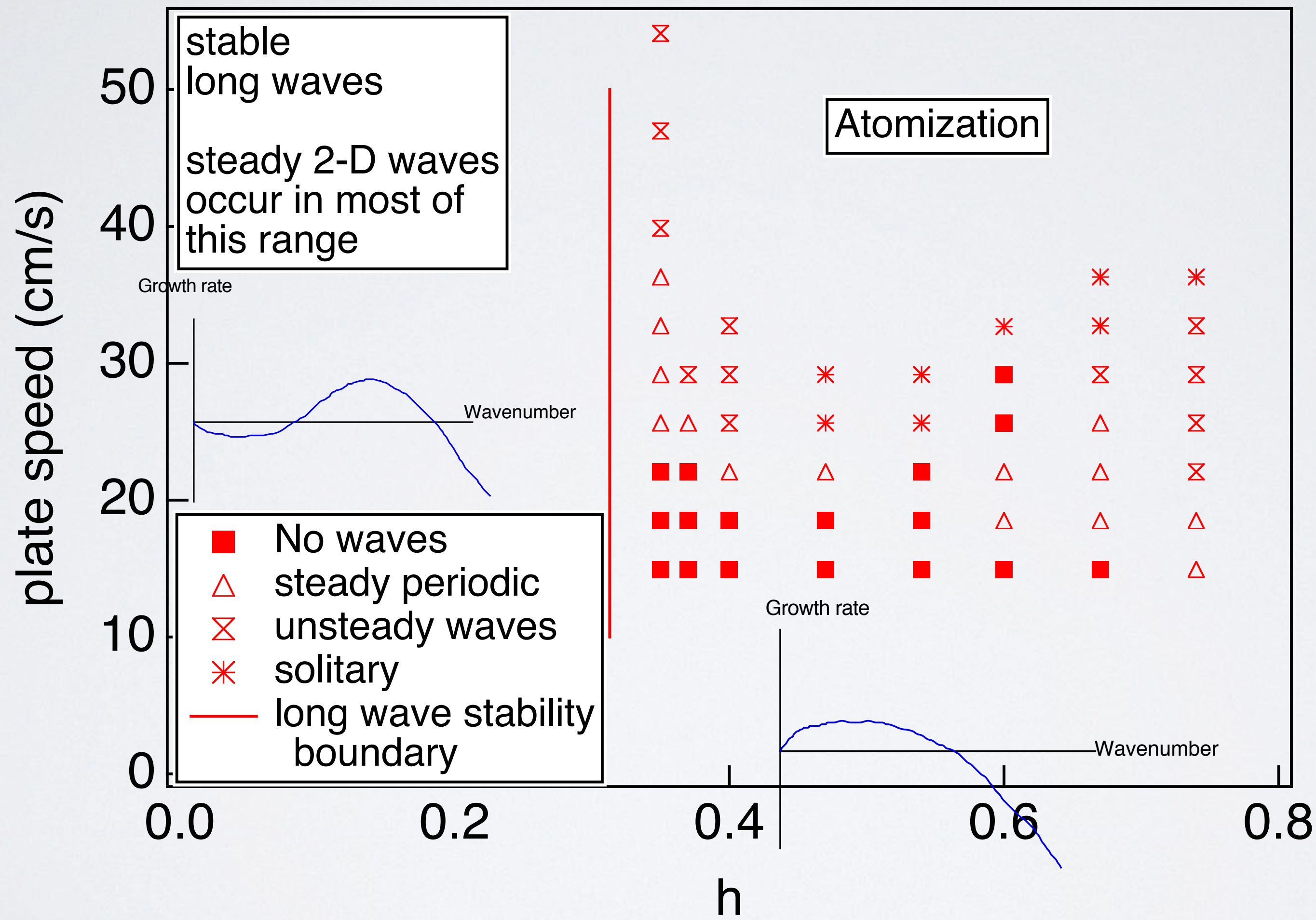

GAS-LIQUID FLOW IN PACKED

DISTURBANCE EVOLUTION WITH DISTANCE IN REACTING SYSTEMS

- "Trickle" bed reactors: pulsing

Enhancing Performance of Three-Phase Catalytic Packed-Bed Reactors

B. A. Wilhite, R. Wu, X. Huang, M. J. McCready and A. Varma

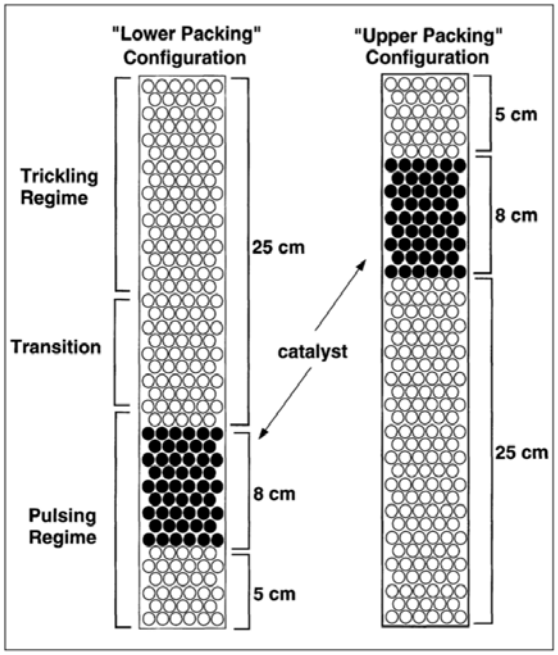

Figure 2. Lower- and upper-packing configurations.

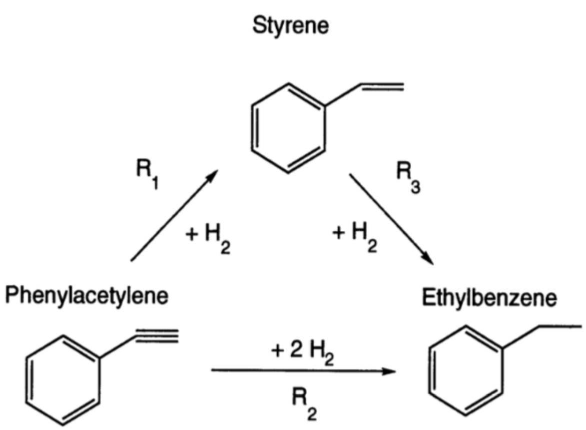

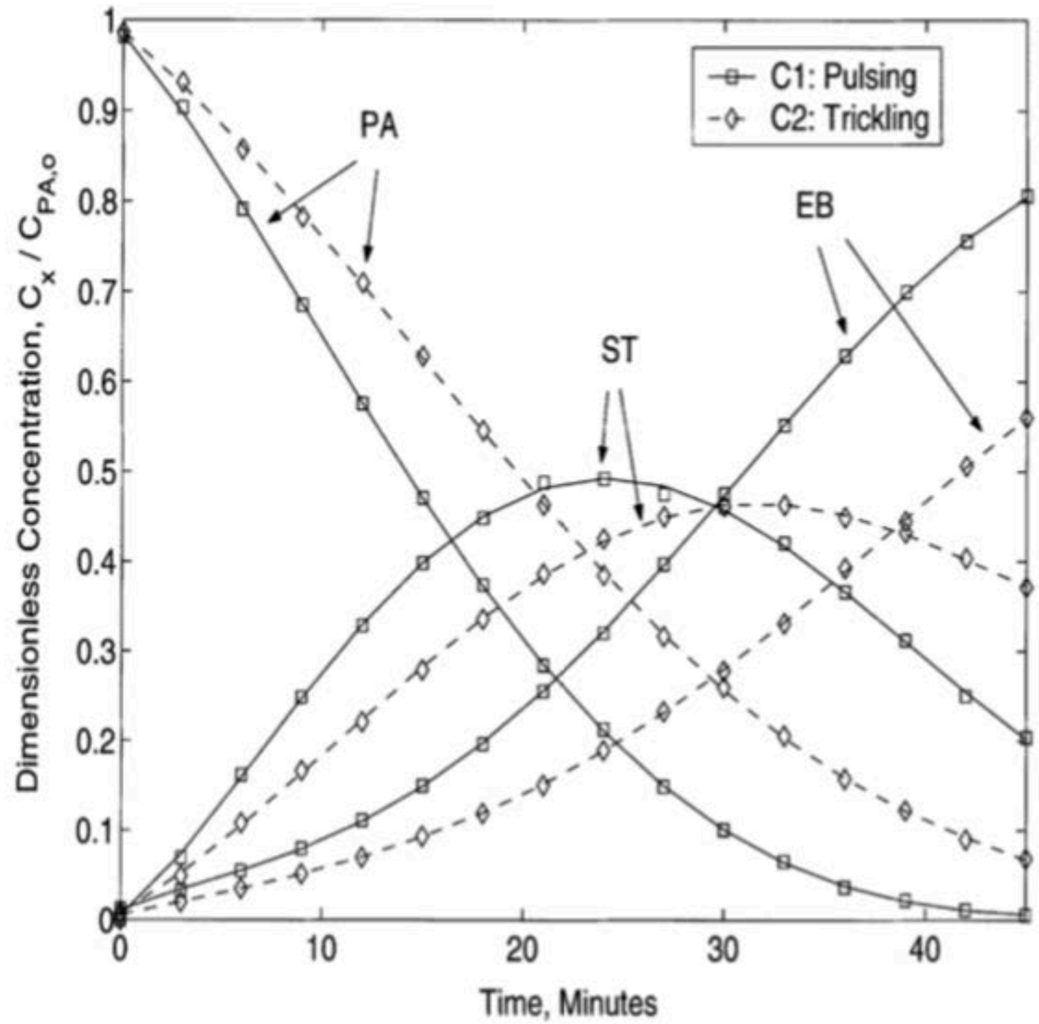

Figure 6. Reactor performance for Series C experiments.

Also studied heat transfer with same idea

FAVORITE PAPER #2

- I wish I had been in the room when these data first were presented to outside researchers!
- There should have been a collective gasp!

MOST STUNNING DATA SET IN ALL OF TURBULENT MASS TRANSFER?

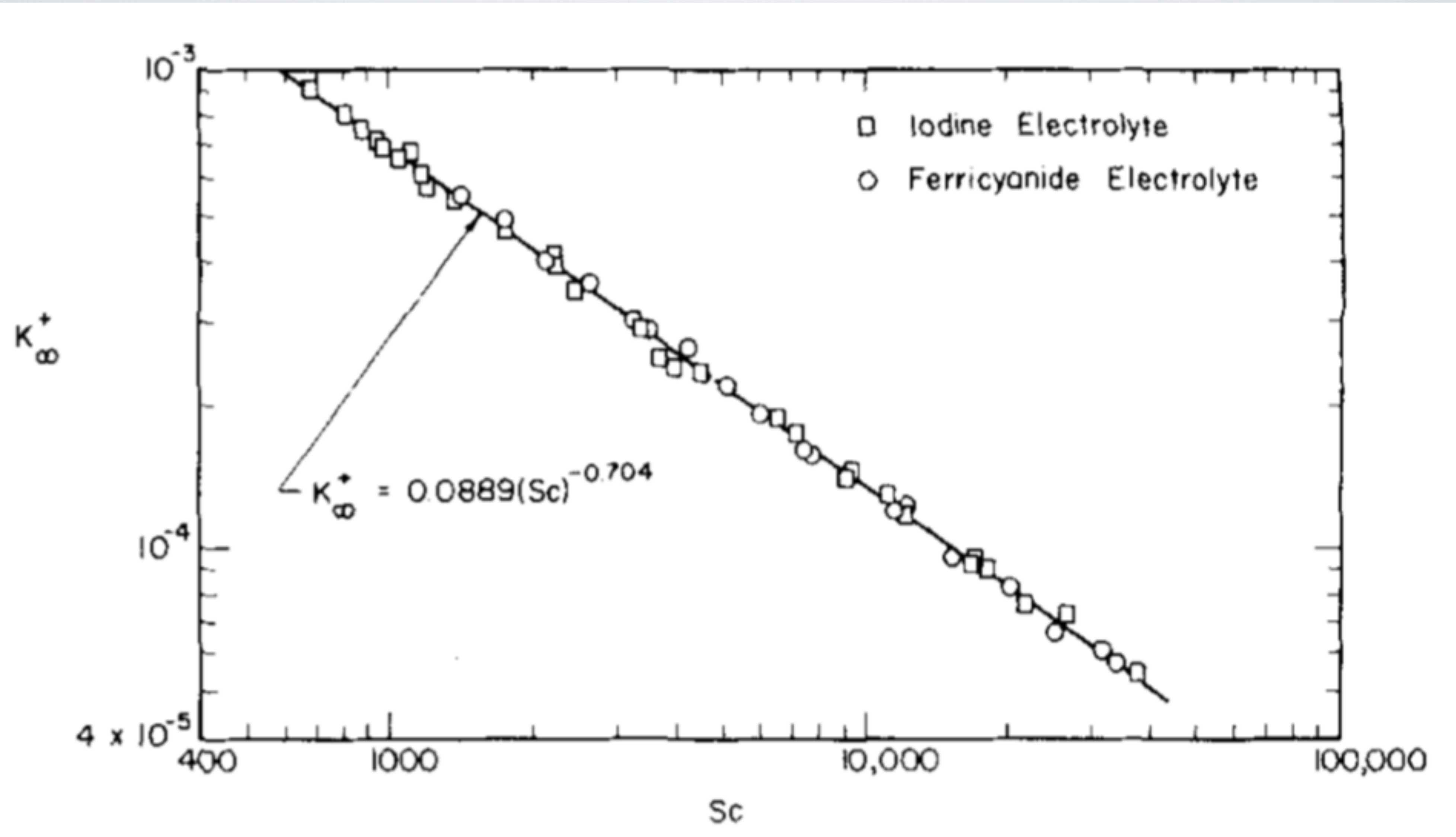

PAPER TWO

Turbulent Mass Transfer Rates to a Wall for Large Schmidt Numbers

DUDLEY A. SHAW
and
THOMAS J. HANRATTY
University of Illinois
Urbana, Illinois

New measurements are presented on the influence of Schmidt number on the rate of mass transfer between a turbulent fluid and a pipe wall. It is found that for large Schmidt numbers the fully developed mass transfer coefficient is related to the friction velocity and the Schmidt number by the equation

$$K_\infty = 0.0889\, v^* \, Sc^{-0.704}$$

The experiments are accurate enough to rule out the $Sc^{-2/3}$ or the $Sc^{-3/4}$ relations commonly used, deduced from plausible limiting expressions for the eddy diffusivity close to a wall. It is argued that these expressions are valid only over a vanishingly small portion of the concentration field as $Sc \to \infty$.

SCOPE

SCALING REMOVES REYNOLDS NUMBER

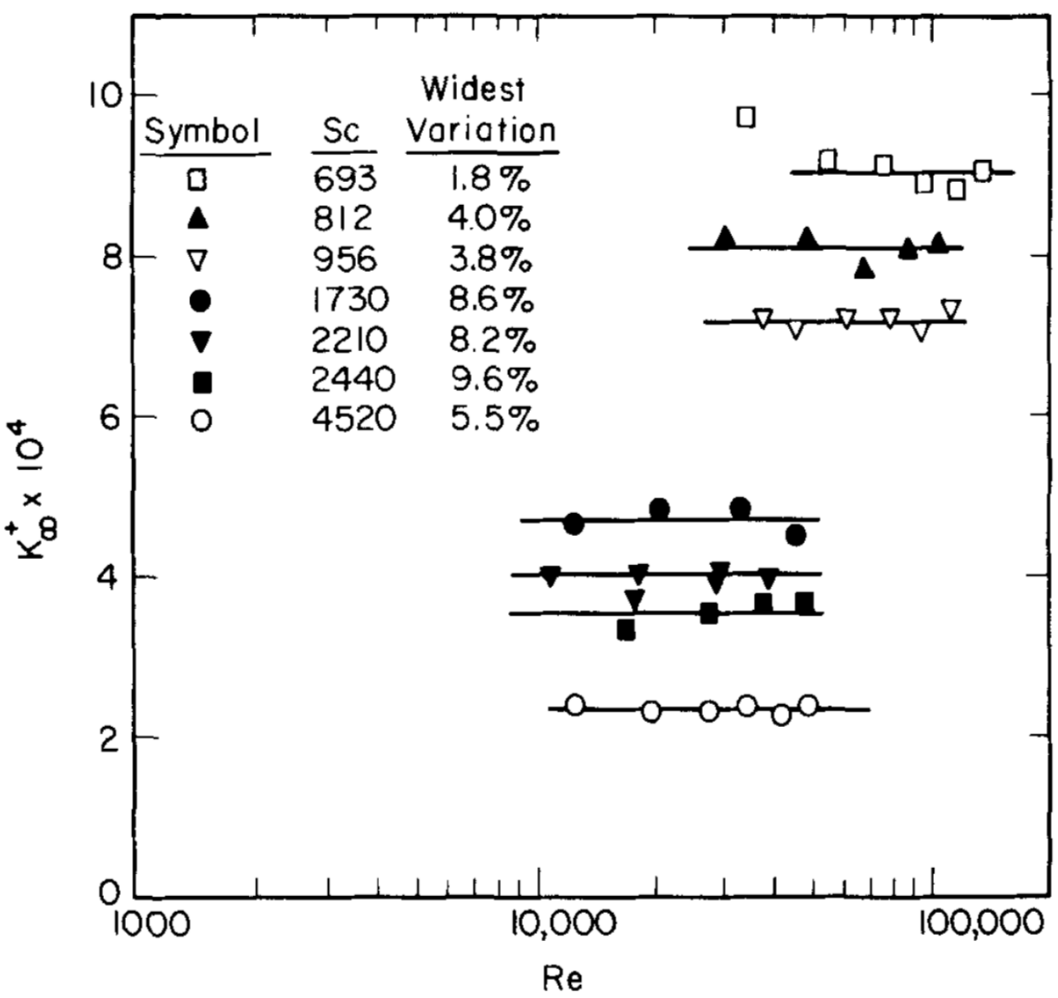

Fig. 7. $K_\infty{}^+$ measured by difference of current (low Schmidt numbers).

DUDLEY A. SHAW
and
THOMAS J. HANRATTY

FIRST: TWO PAGES OF ANALYSIS!

THEORY

The Use of Eddy Diffusion Coefficients

A number of researchers have assumed that (14) is valid throughout the concentration field and that the correlation coefficient R is independent of Schmidt number to argue

$$\delta_L^+ \sim Sc^{-1/2} \quad (21)$$

Since $\delta_c^+ \sim Sc^{-1/3 \text{ or } -1/4}$, it follows that $\delta_L^+/\delta_c^+ \rightarrow 0$ as

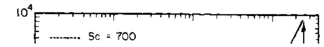

$$\frac{\partial c}{\partial t} + \overline{U}\frac{\partial c}{\partial x} + v\frac{d\overline{C}}{dy} + u\frac{\partial \overline{C}}{\partial x} = D\left(\frac{\partial^2 c}{\partial y^2} + \frac{\partial^2 c}{\partial x^2} + \frac{\partial^2 c}{\partial z^2}\right)$$

$$- \frac{\partial}{\partial x}(uc) - \frac{\partial}{\partial y}(vc - \overline{vc}) - \frac{\partial}{\partial z}(wc) \quad (19)$$

by the first term of a Taylor series in y. Thus, as shown in pages 279-282 of the book by Monin and Yaglom (1965) the time average, the component of the turbulent velocity fluctuations perpendicular to the wall, and the turbulent eddy viscosity are given as

$$\overline{U} = v^* y^+ \quad (8)$$

$$v' = (\overline{v^2})^{1/2} = k_1 v^* y^{+2} \quad (9)$$

$$\frac{\nu_T}{\nu} = k_2 y^{+3} + k_3 y^{+4} \quad (10)$$

If it is assumed that turbulent mass transport is analogous to momentum transport in that ϵ is proportional to ν_T, then it would follow that either $\epsilon \sim y^{+3}$ or $\epsilon \sim y^{+4}$, depending on whether $k_2 = 0$.

Another theoretical approach for estimating the exponent in (4) is to use a Taylor series expansion of the concentration field as well as the velocity field. Then

$$c' = (\overline{c^2})^{1/2} = k_4 \frac{d\overline{C}}{dy}\bigg|_{\text{wall}} y \quad (11)$$

where k_4 is a proportionality constant. The eddy diffusivity can be related to the fluctuating concentration and velocity field by using a Reynolds transport coefficient

$$\overline{vc} = -\epsilon(y)\frac{d\overline{C}}{dy} \quad (12)$$

Since

$$\overline{vc} = R\, v' c' \quad (13)$$

where R is the correlation coefficient for $y \rightarrow 0$, it follows that the limiting behavior of $\epsilon(y)$ for $y \rightarrow 0$ is

$$\epsilon^+ = \frac{\epsilon(y)}{\nu} = -R\, k_1 k_4\, y^{+3} \quad (14)$$

$$\delta_c^+ = \frac{1}{K^+ Sc} \quad (18)$$

where $\delta_c^+ = \delta_c v^*/\nu$. Consequently, $\delta_c^+ \sim Sc^{-p}$, with $1/4 < p < 1/3$. The differential equation describing the concentration fluctuation is obtained from the mass balance equation as indicated by Hinze (1959):

$$\frac{\partial c}{\partial t} + \overline{U}\frac{\partial c}{\partial x} + v\frac{d\overline{C}}{dy} + u\frac{\partial \overline{C}}{\partial x} = D\left(\frac{\partial^2 c}{\partial y^2} + \frac{\partial^2 c}{\partial x^2} + \frac{\partial^2 c}{\partial z^2}\right)$$

$$- \frac{\partial}{\partial x}(uc) - \frac{\partial}{\partial y}(vc - \overline{vc}) - \frac{\partial}{\partial z}(wc) \quad (19)$$

The orders of magnitude of several of the terms appearing in this equation have been examined by Sirkar and Hanratty (1970). They showed that for large Schmidt numbers, $\partial^2 c/\partial y^2$ is large compared to $\partial^2 c/\partial x^2$ and $\partial^2 c/\partial z^2$ and that $\partial c/\partial t$ is large compared to $\overline{U}(\partial c/\partial x)$ or $u(\partial \overline{C}/\partial x)$. Equation (19) then simplifies to

$$\frac{\partial c^+}{\partial t^+} + v^+\frac{d\overline{C}^+}{dy^+} = \frac{1}{Sc}\left(\frac{\partial^2 c^+}{\partial y^{+2}}\right) - \frac{\partial}{\partial x^+}(u^+c^+)$$

$$- \frac{\partial}{\partial z^+}(w^+c^+) - \frac{\partial}{\partial y^+}(v^+c^+ - \overline{v^+c^+}) \quad (20)$$

where t, y, u, v, and w have been made dimensionless using wall parameters v^* and ν. $\overline{C}$ and c have been made dimensionless using C_B. The term $(1/Sc)(\partial^2 c^+/\partial y^{+2})$ which governs the influence of molecular diffusion should be of prime importance close to the wall and therefore should play a role in determining the limiting behavior of $\overline{vc}$ as $y \rightarrow 0$. Since the transient term $\partial c^+/\partial t^+$ is of the same order as $(1/Sc)(\partial^2 c^+/\partial y^{+2})$ close to the wall, we conclude that the thickness of the region over which the limiting relation for the eddy diffusivity is valid has the dependency

∂y^{+2}). For large y^+, the molecular diffusion term is negligible and $\hat{c}$ varies in a way similar to that suggested by Levich in (15):

$$\hat{c} = -\frac{\hat{v}}{i\omega^+} y^{+2} \frac{d\overline{C}^+}{dy^+} \quad (27)$$

A solution to (26) has been presented by Shaw (1976) and by Shaw and Hanratty (1977) for the boundary conditions that $\hat{c} = 0$ at $y^+ = 0$ and as $y^+ \rightarrow \infty$. The amplitude of the concentration fluctuations is given as $|\hat{c}| = (\hat{c}\hat{c}^*)^{1/2}$, where c^* is the complex conjugate of c. The ratio $\dfrac{|\hat{c}|}{|\hat{v}|\dfrac{d\overline{C}^+}{dy^+}}$ calculated from (26) for $\omega^+ = 0.0628$ and for $\epsilon^+ = 0.00032y^{+4}$ is shown in Figure 1, where the distance from the wall has been normalized with respect to $\delta_c^+ \sim (1/Sc^{1/4})$. The value of ω^+ used in this calculation was taken as the median frequency of the fluctuations of u in the viscous sublayer determined from the measurements of Lee (1968). The calculated amplitude was found to be independent of the form chosen for ϵ^+. The same profile was obtained for $\epsilon^+ = 0.000463y^{+3.38}$.

One of the results of this calculation is that as $y^+ \rightarrow 0$

$$\overline{v^+c^+} = -\sqrt{2}\, Sc^{1/2}\, \overline{K}^+\, y^{+3} \int_0^\infty \frac{W_v}{\omega^{+3/2}}\, d\omega^+ \quad (28)$$

or that

$$\epsilon^+ = \frac{\sqrt{2}\, y^{+3}}{Sc^{1/2}} \int_0^\infty \frac{W_v}{\omega^{+3/2}}\, d\omega^+ \quad (29)$$

This is consistent with (14), but, contrary to the assumption usually made, the coefficient is found to depend on Schmidt number. The solid line in Figure 1 is (27),

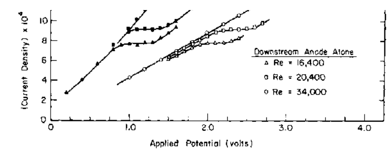

Fig. 2. Polarization curves for different anode configurations at $Sc = 695$.

and the broken lines represent the region where the concentration fluctuations are affected by molecular diffusion. These show the linear dependency on y^+ at small y^+ given by (11). If the edge of the concentration boundary layer is defined as $\overline{C}/C_b = 0.99$, then it is located at the value of $y^+(Sc)^{1/4}$ indicated by the arrow in Figure 1. From Figure 1 it is seen that the fraction of the concentration boundary layer over which molecular diffusivity is influencing the concentration fluctuations becomes progressively smaller as the Schmidt number increases.

Of particular interest is the result that for $Sc \rightarrow \infty$ the variation of the concentration fluctuation over almost all of the concentration boundary layer is not influenced by molecular diffusion. That is, it is given by (27). This would suggest that the eddy diffusion coefficient for $Sc \rightarrow \infty$ should be represented by an equation of the form

$$\epsilon^+ = g(y^+) \quad (30)$$

If the simplified version of the mass balance Equation (22) were valid, we would get

$$g(y^+) \sim y^{+4} \quad (31)$$

as suggested by Levich. However, there is no reason to expect that the nonlinear terms in (20) are negligible for large y^+. Consequently, we must anticipate that $g(y^+)$ could be more complicated than the Levich relation.

MOST STUNNING DATA SET IN ALL OF TURBULENT MASS TRANSFER?

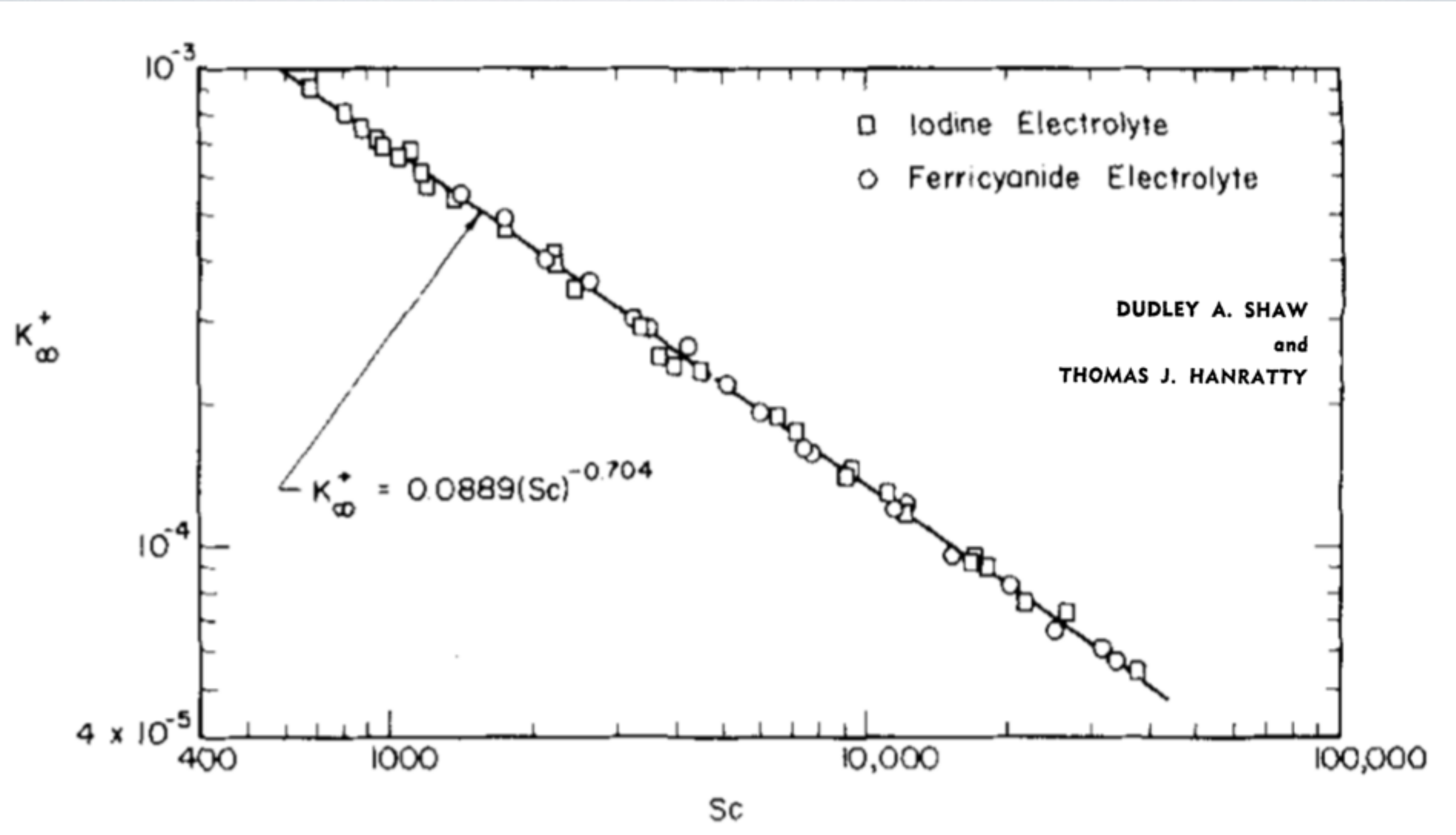

WARREN STEWART TAKES A SHOT AT WHY!

Not this!

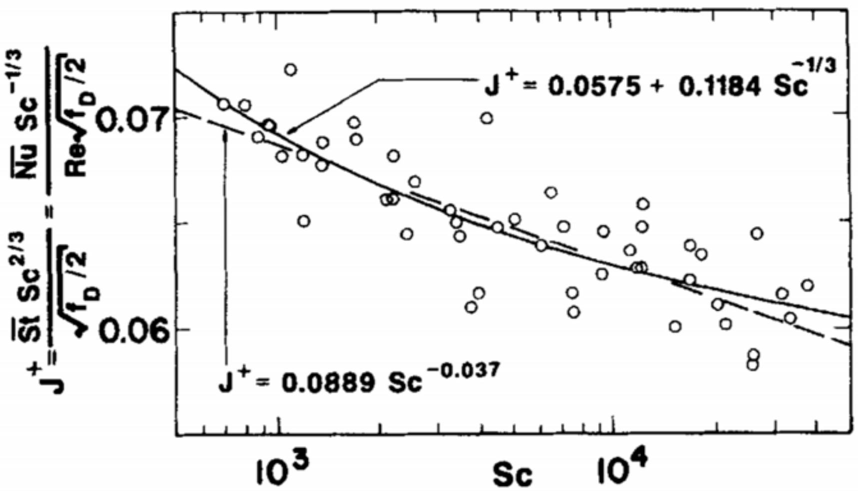

Figure 7. Correlations of data of Shaw and Hanratty (1977a) for turbulent mass transfer in pipes.
---- Shaw and Hanratty fitted power function
— fitted two-term version of Eq. 52

Forced Convection: IV. Asymptotic Forms for Laminar and Turbulent Transfer Rates

Mass transfer rates in laminar and turbulent nonseparated boundary layers are asymptotically expanded for small values of the diffusivity $\mathcal{D}_{AB}$, with a uniform state on the mass transfer surface. Results for heat transfer follow by analogy. The thermal or binary Nusselt number at small net mass transfer rates is given asymptotically by a generalized penetration expression

$$\langle Nu \rangle = a_{00}Pe^{1/2} + a_{01}Pe^0 + \cdots \qquad \text{(A)}$$

for short times, or for boundary layers that duplicate the surface tangential motion. For flows past rigid interfaces, the long-time average of $\langle Nu \rangle$ is given asymptotically by a generalized Chilton-Colburn relation

$$\langle \overline{Nu} \rangle = b_{00}Pe^{1/3} + b_{01}Pe^0 + \cdots \qquad \text{(B)}$$

W. E. Stewart
Department of Chemical Engineering
University of Wisconsin
Madison, Wisconsin 53706

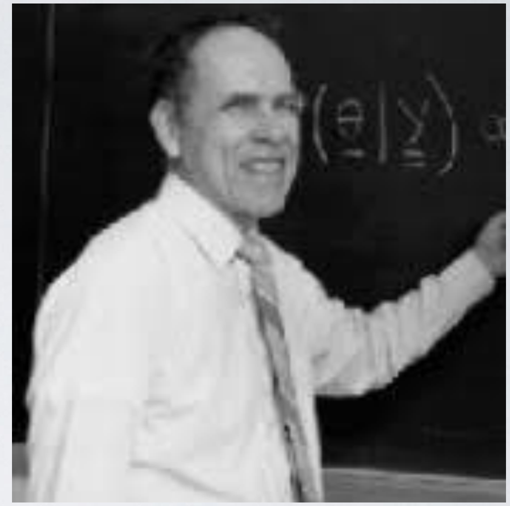

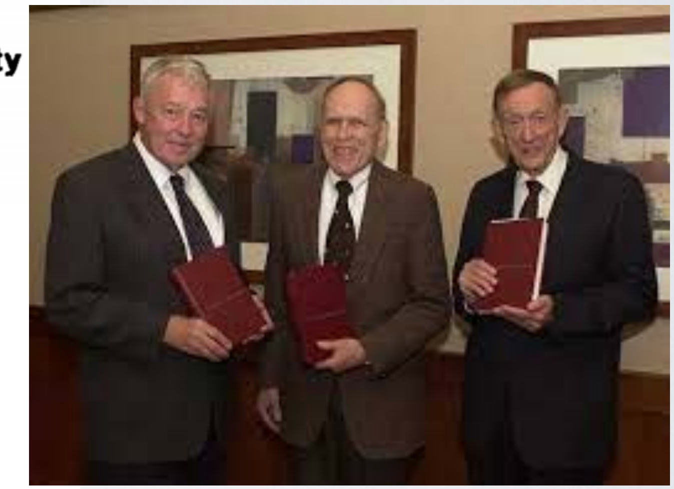

AIChE Journal **December 1987 Vol. 33, No. 12**

HIGH FREQUENCIES ARE "FILTERED"

Influence of Schmidt Number on the Fluctuations of Turbulent Mass Transfer to a Wall

DUDLEY A. SHAW
and
THOMAS J. HANRATTY
University of Illinois
Urbana, Illinois 61801

Measurements are presented on the influence of Schmidt number on the frequency of the mass transfer fluctuations at a solid boundary. The shape of the spectral function is similar at all Schmidt numbers. A relation between the mass transfer fluctuations and the fluctuating velocity field can be obtained only at high frequencies. A comparison of the scale and the frequency of the mass transfer fluctuations and the velocity fluctuations suggests that the rate of mass transfer is controlled by convective motions in the flow oriented eddies described by a number of previous investigators. However, the concentration fluctuations caused by these convective motions are greatly dampened close to the wall by molecular diffusion. Thus the mass transfer fluctuations reflect only the scale and not the frequency of the convective motions in the flow oriented eddies.

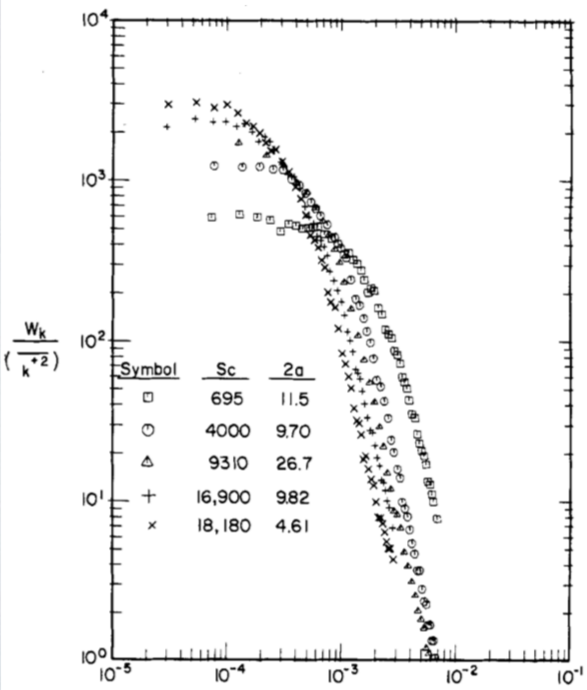

Fig. 7. Effect of Schmidt number on the mass transfer spectrum.

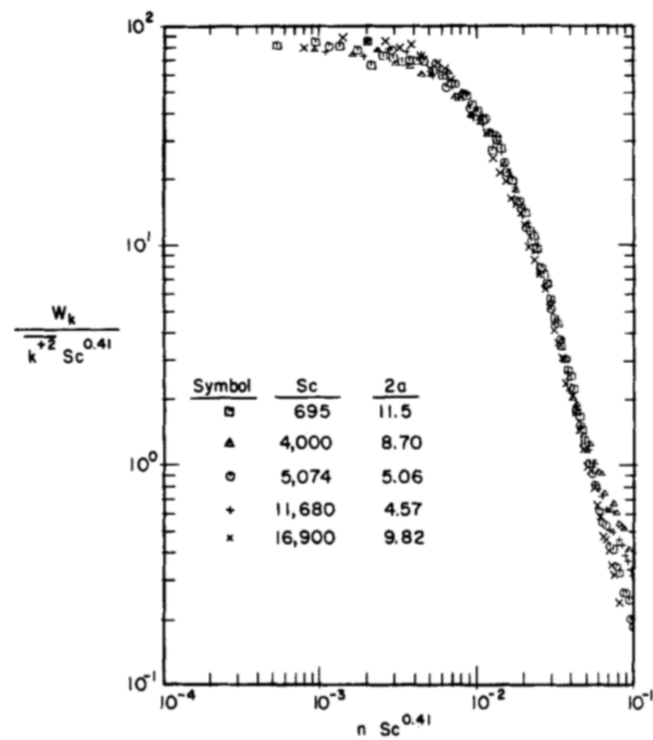

Fig. 8. Spectra plotted to show similarity in shape.

Mechanism of Turbulent Mass Transfer at a Solid Boundary

Mass transfer between a turbulent fluid and a solid boundary is considered for the case of large Schmidt numbers. The variation of the mass transfer coefficient with time, *K(t)*, is calculated by solving the mass balance equation using a random velocity input. An interpretation of the mass transfer process which is radically different from that given by classical approaches is obtained.

J. A. CAMPBELL and
T. J. HANRATTY
University of Illinois
Urbana, IL 61801

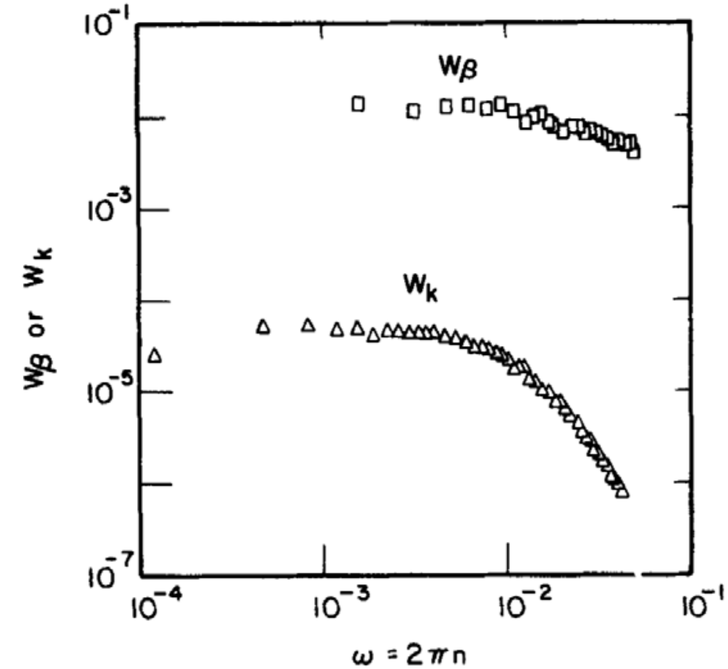

Figure 1. Spectral density functions for β and k from experimental measurements.

SO WHAT IS GOING ON?

We know the equation $$\frac{\partial C}{\partial t} + v\frac{\partial C}{\partial y} + w\frac{\partial C}{\partial z} = \frac{1}{S}\frac{\partial^2 C}{\partial y^2},$$

- "Boundary-Layer arguments (as in Prandtl) suggest that convection and diffusion must <u>balance</u> near the wall.
- Numerical simulations by Back and McCready (1988) indicate that only the term with normal velocity is causing <u>net</u> transport.
- Continuity equation requires that $v \sim y^2$
- All of this leads to $K \sim S^{-2/3}$ not -.704
- Ex: Rotating disk, Thermal Boundary-Layer

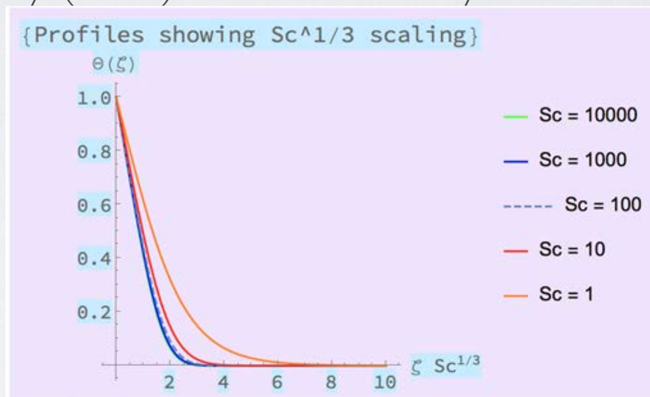

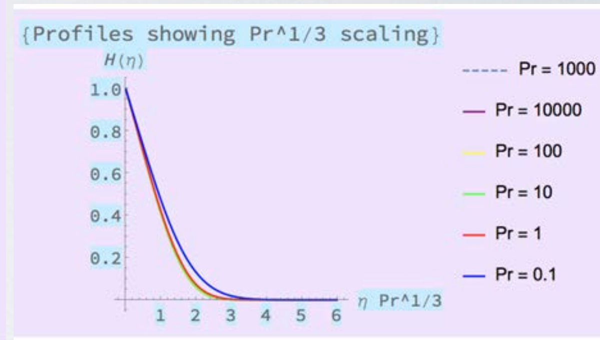

- … First part is easy. The mass transfer coefficient is non-dimensioqnalized with v*. The friction velocity scales with "all" of the energy in the flow.
  - However, as Tom and multiple students have told us, the mass transfer boundary layer is essential a low-pass filter so that much of the "energy" of the flow is not effective in cause mass transfer…
    - Hence K/v* should fall off more quickly with S than -2/3.
- Why "perfect" power law for such a large range? and why -.704?
- God wanted it this way!

CONVECTION AND DIFFUSION TIME SCALES MUST BALANCE

Shear Enhanced Transport in Oscillatory Liquid Membranes

David T. Leighton, Jr.,
Mark J. McCready
Department of Chemical Engineering
University of Notre Dame
Notre Dame, IN 46556

Can reduce membrane diffusion resistance from length of pore to just radius of pore by correct choice of oscillation frequency

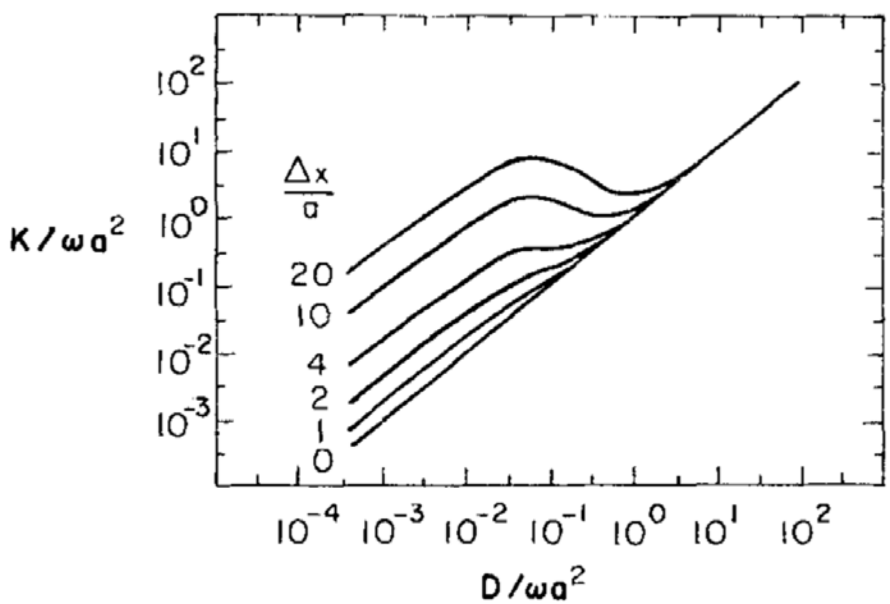

Figure 3. Plot of effective diffusivity vs. molecular diffusivity.

United States Patent [19] — [11] **Patent Number: 4,994,189**
Leighton et al. — [45] **Date of Patent: Feb. 19, 1991**

[54] **SEPARATION DEVICE UTILIZING OSCILLATORY LIQUID MEMBRANE**

[76] Inventors: **David T. Leighton,** 60049 Cedar Rd., Mishawaka, Ind. 46544; **Mark J. McCready,** 54155 E. Lake Dr., South Bend, Ind. 46635

[21] Appl. No.: **252,575**

[22] Filed: **Sep. 30, 1988**

[51] **Int. Cl.**[5] **B01D 61/38**

[52] **U.S. Cl.** **210/637; 210/643; 210/321.84**

[58] **Field of Search** 210/643, 644, 649, 637, 210/321.84; 261/122

Mechanics at University of Canterbury, Christchurch, New Zealand, Dec. 9-13, 1974.

Richard G. Rice and L. C. Eagleton, *Mass Transfer Produced by Laminar Flow Oscillations,* The Canadian Journal of Chemical Engineering 48, pp. 46-51, Feb. 1970.

Richard G. Rice, *Diffusive Mass Transfer Produced by Laminar Flow Oscillations,* A Dissertation in Chemical Engineering, Presented to the Faculty of the Graduate School of Arts and Sciences of the University of Pennsylvania, 1968.

Gary W. Howell, *Separation of Isotopes by Oscillatory Flow,* Phys. Fluids 31 (6), pp. 1803-1805 (Jun. 1988).

U. H. Kurzweg and Ling de Zhao, *Heat Transfer by High-Frequency Oscillations: A New Hydrodynamic*

U.S. Patent — **Feb. 19, 1991** — **Sheet 1 of 3** — **4,994,189**

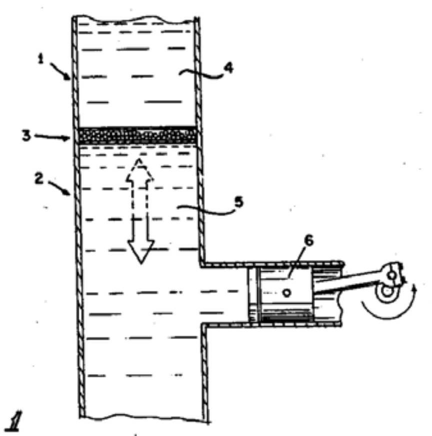

FIG. 1

POSSIBLE APPLICATION TO BONE TISSUE

- Your bones respond to stresses by growing larger and more dense.
    - Dramatic effect in various athletes.
    - Effect known for a century, "Wolff's Law" — osteocytes are sensitive to stress and respond chemically.
- Is this the entire story?
- How come humans suffer considerable bone mass loss with continuous exposure to microgravity?

ELSEVIER

Journal of Biomechanics 38 (2005) 2337–2343

JOURNAL OF BIOMECHANICS

www.elsevier.com/locate/jbiomech
www.JBiomech.com

Effect of oscillating fluid shear on solute transport in cortical bone

Stephanie M. Schmidt, Mark J. McCready, Agnes E. Ostafin*

Department of Chemical and Biomolecular Engineering, 182 Fitzpatrick Hall, University of Notre Dame, Notre Dame, IN 46556-5637, USA

Accepted 14 October 2004

CHE 487: WIDER IMPLICATIONS

CEE chemical engineering educat

FALL 1969

Graduate Education Issue

AMUNDSON . . . . Why Mathematics?
CHURCHILL . . Momentum and Energy Transfer
DOUGHARTY & SMITH . . . . . Reactor Design
HANRATTY . . . . Fluid Dynamics
HULBURT . . . . Particulate Systems
LAPIDUS . . . . Optimal Control
LIGHTFOOT . . . . Diffusional Operations
MARTIN . . . . Thermodynamics
PRAUSNITZ . . . . Phase Equilibria

Also **HOUGEN** Remembers **A. P. COLBURN**
GRINTER Writes on Accreditation
MORGEN Reviews the Curriculum
WEBER On Subscription Policy

CHEMICAL ENGINEERING DIVISION OF AMERICAN SOCIETY FOR ENGINEERING EDUCATION

A Course in Momentum Transport

FLUID DYNAMICS

THOMAS J. HANRATTY
University of Illinois
Urbana, Illinois 61801

Fluid dynamics plays a central role in many problems of interest to chemical engineers. Because of this, the semester course in the area presented by the ChE Division of the University of Illinois has been one of the most durable offerings in its graduate curriculum. I have taught this course since 1953 and one similar to it had existed many years prior to my involvement.

Thomas J. Hanratty is professor of chemical engineering at University of Illinois. He was educated at Villanova, Ohio State, and Princeton University, PhD ('53). His recent professional honors include the Curtis W. McGraw Award (ASEE) and the William H. Walker and the Professional Prograss Awards of AIChE.

CHE 487

FLUID DYNAMICS

ChE 487
Spring 1988
Prof. T. J. Hanratty

1 unit

I. Introductory Remarks

A. Application of Thermodynamics to Fluid Dynamics Problems
B. Application of Newton's Second Law to a Flow Field
1. Momentum Theorem
2. Energy Theorem

II. Review of Uni-Directional Flow Problems and Newton's Law of Viscosity

A. Pipe Flow
1. Convention of Shear Stress
B. Couette Flow Between Rotating Cylinders - Viscometric Equations
C. Kinetic Theory Interpretation (Momentum Flux vs Shear Stress)

III. Development of the Equations for a 3-D Flow Field

A. Continuity Equations
B. Momentum Theorem Applied
1. Body Forces
2. Surface Forces
C. Properties of the Stress Tensor, τ
D. Velocity Gradient Tensor, $\varepsilon_{ij} + \Omega_{ij}$
E. Generalized Constituative Relations
1. Generalization of Newton's Law of Viscosity (for a Newtonian Fluid)
2. Navier-Stokes Equations

IV. Status of Non-Newtonian Fluid Mechanics

A. Non-Linear Effects
B. Normal Stress Effects
C. Viscoelastic (Time) Effects
D. Maxwell's Linear Viscoelastic Model
E. Reiner-Revlin Model
F. Oldroyd's Convective Derivative

V. Discussion of the Navier-Stokes Equation

VI. Creeping Flow

A. Flow Around a Solid Sphere (Stokes' Problem)
B. Whitehead's Paradox (Regular Perturbation Technique)
C. Stokes' Paradox (Flow Around a Cylinder)
D. Recent Developments
1. Oseens' Approximation (Cylinder and Sphere)
2. Singular Perturbation Techniques

VII. Ideal Flow Theory - Euler Equation of Motion

A. Assumption of Irrotationality
B. Bernoulli Equation
C. Incompressible Potential Flow Problems
1. Flow Around a Sphere
2. Wave Motion
D. Two-Dimensional, Inviscid Flow (Complex Variables)
1. Flow Around a Cylinder
2. 2-D Vortex
3. Flow around a Cylinder with Circulation
4. Conformed Mapping
a. Flow Around a Cylinder
b. Flow Around a Flat Plate
c. Free-Streamline Problems
d. Schwarz-Christoffel Transformation - Flow Through 2-D Orifice

VIII. Boundary Layer Theory

A. Physical Assumptions
B. Equations of the Boundary (2-D)
C. Typical Problem Definitions for BLT
D. Remarks on Separation
E. Examples of BLT
1. Flow Over a Flat Plate
2. Stagnation Flow
3. Remarks on Similarity Solutions
4. Blasius' Series Solution
a. Gortler's Expansion
5. Integral Methods (Approximate Methods)
a. Flow Over a Flat Plate
b. Pohlhausen Method
c. Bohlen-Walz Improvement
F. Numerical Solutions of the Boundary Layer Equations

IX. Turbulence

A. Reynolds Stresses
B. Empirical Approaches (Mixing Length Theories)
C. Dimensional Analysis Approach: law of the wall, defect law, overlap law
D. Equation for Turbulent Energy
E. Modern Methods for Predicting Reynolds Stresses
1. Zero Equation Models
2. One Equation Models
3. Two Equation Models
4. Direct Solution of the Equation for Reynolds Stress

X. Numerical Methods

TJH:klj
11/87

TOP OF FOOD CHAIN!

Tom was an Advisory Editor for Prentice Hall

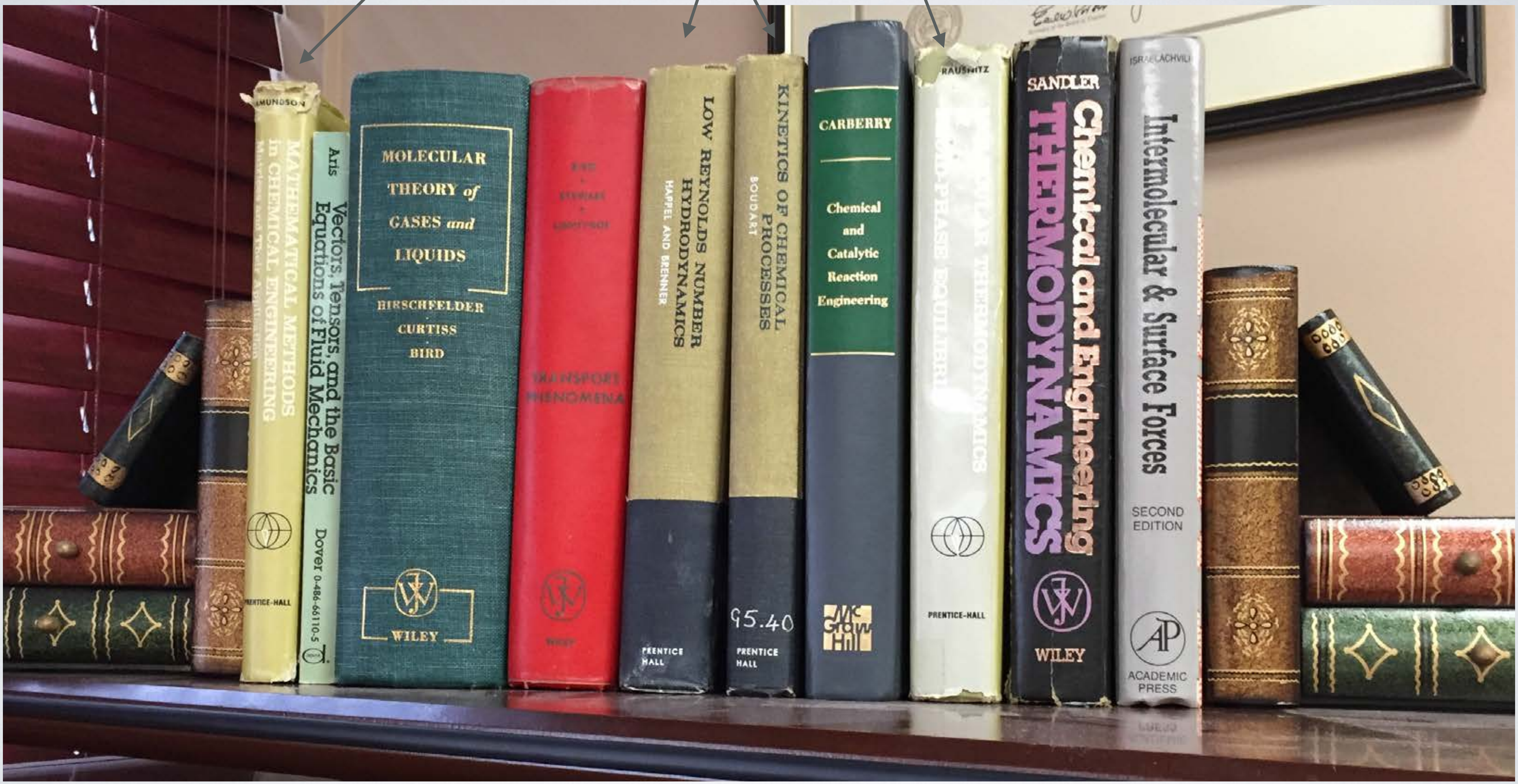

FORTUNE "30", 1980 — 2016

1980 Full list — Current View: 1-100

Rank	Company	Revenues ($ millions)	Profits ($ millions)
1	Exxon Mobil	79,106.5	4,295.2
2	General Motors	66,311.2	2,892.7
3	Mobil	44,720.9	2,007.2
4	Ford Motor	43,513.7	1,169.3
5	Texaco	38,350.4	1,759.1
6	ChevronTexaco	29,947.6	1,784.7
7	Gulf Oil	23,910.0	1,322.0
8	Intl. Business Machines	22,862.8	3,011.3
9	General Electric	22,460.6	1,408.8
10	Amoco	18,610.3	1,506.6
11	ITT Industries	17,197.4	380.7
12	Atlantic Richfield	16,234.0	1,165.9
13	Shell Oil	14,431.2	1,125.6
14	U.S. Steel	12,929.1	-293.0
15	Conoco	12,648.0	815.4
16	DuPont	12,571.8	938.9
17	Chrysler	12,001.9	-1,097.3
18	Tenneco Automotive	11,209.0	571.0
19	AT&T Technologies	10,964.1	635.9
20	Sunoco	10,666.0	699.9
21	Occidental Petroleum	9,554.8	561.6
22	ConocoPhillips	9,502.8	891.1
23	Procter & Gamble	9,329.3	577.3
24	Dow Chemical	9,255.4	783.9
25	Union Carbide	9,176.5	556.2
26	United Technologies	9,053.4	325.6
27	Navistar International	8,392.0	369.6
28	Goodyear Tire & Rubber	8,238.7	146.2
29	Boeing	8,131.0	505.4
30	Eastman Kodak	8,028.2	1,000.8

1	Walmart	$482,130
2	Exxon Mobil	$246,204
3	Apple	$233,715
4	Berkshire Hathaway	$210,821
5	McKesson	$181,241
6	UnitedHealth Group	$157,107
7	CVS Health	$153,290
8	General Motors	$152,356
9	Ford Motor	$149,558
10	AT&T	$146,801
11	General Electric	$140,389
12	AmerisourceBergen	$135,962
13	Verizon	$131,620
14	Chevron	$131,118
15	Costco	$116,199
16	Fannie Mae	$110,359
17	Kroger	$109,830
18	Amazon.com	$107,006
19	Walgreens Boots Alliance	$103,444
20	HP	$103,355
21	Cardinal Health	$102,531
22	Express Scripts Holding	$101,752
23	J.P. Morgan Chase	$101,006
24	Boeing	$96,114
25	Microsoft	$93,580
26	Bank of America Corp.	$93,056
27	Wells Fargo	$90,033
28	Home Depot	$88,519
29	Citigroup	$88,275
30	Phillips 66	$87,169

CONCLUSIONS

- Just two examples of a couple hundred papers
  - Ground breaking approaches
  - Value well beyond specific example
  - Results of continuing value
- Tom was one of the best people in the "top of the food-chain" field of engineering
  - Intrinsic quality of the research,
  - intellectual depth and broad utility and of educational core
  - relevance to developing industrial sectors
- Can we stay there?

POSTLUDE

- We could "scale up" these:

HEALTH

F.D.A. Approves Second Gene-Altering Treatment for Cancer

By DENISE GRADY OCT. 18, 2017

HEALTH

F.D.A. Approves First Gene-Altering Leukemia Treatment, Costing $475,000

By DENISE GRADY AUG. 30, 2017